He, C., Xiao, P., Zhang, L., Mao, J., Cao, A. and Nikitopoulos, K. (2018) Efficient DCT-MCM Detection for Single and Multi-Antenna Wireless Systems. In: 28th Annual IEEE International Symposium on Personal, Indoor and Mobile Radio Communications (IEEE PIMRC 2017), Montreal, QC, Canada, 08-13 Oct 2017, ISBN 9781538635315 (doi:10.1109/PIMRC.2017.8292604)

# Efficient DCT-MCM Detection for Single and Multi-Antenna Wireless Systems

Chang He[1], Pei Xiao[1], Lei Zhang[2], Juquan Mao[1], Aijun Cao[3], and Konstantinos Nikitopoulos[1]

[1]Institute for Communication Systems, University of Surrey, United Kingdom, GU2 7XH
[1]{c.he, p.xiao, juquan.mao, k.nikitopoulos}@surrey.ac.uk,
[2]School of Engineering, University of Glasgow, Glasgow, G12 8QQ, UK
[2]Lei.Zhang@glasgow.ac.uk
[3]ZTE Wistron Telecom AB, Stockholm, Sweden, 164 51 Kista
[3]cao.aijun@zte.com.cn

***Abstract*—The discrete cosine transform (DCT) based multicarrier modulation (MCM) system is regarded as one of the promising transmission techniques for future wireless communications. By employing cosine basis as orthogonal functions for multiplexing each real-valued symbol with symbol period of $T$, it is able to maintain the subcarrier orthogonality while reducing frequency spacing to $1/(2T)$ Hz, which is only half of that compared to discrete Fourier transform (DFT) based multicarrier systems. In this paper, following one of the effective transmission models by which zeros are inserted as guard sequence and the DCT operation at the receiver is replaced by DFT of double length, we reformulate and evaluate three classic detection methods by appropriately processing the post-DFT signals both for single antenna and multiple-input multiple-output (MIMO) DCT-MCM systems. In all cases, we show that with our reformulated detection approaches, DCT-MCM schemes can outperform, in terms of error-rate, conventional OFDM-based systems.**

***Index Terms*—Discrete cosine transform (DCT), signal-to-noise ratio (SNR) analysis, multiple-input multiple-output (MIMO), frequency-selective channel, equalizer design.**

## I. Introduction

As a promising complementary waveform for the next generation wireless communications, the discrete-cosine-transform (DCT) based multicarrier modulation (MCM) adopts the cosinusoidal orthogonal functions $\cos(2\pi \times kt/(2T))$ to achieve a subcarrier spacing of $1/(2T)$ Hz, with $k$ being the sub-channel index and $T$ being the symbol duration respectively, but under the restriction that only real-valued signals are transmitted [1].

Correspondingly, the multiplexing and de-multiplexing of sub-carriers can be simply implemented by using the inverse discrete cosine transform (IDCT) and DCT, instead of the inverse discrete Fourier transform (IDFT) pairs in orthogonal frequency division multiplexing (OFDM) [2], [3], [4] widely used in 4G systems and its variants proposed for 5G, such as generalized frequency division multiplexing (GFDM) [5], universal filtered multi-carrier (UFMC) [6], [7], filtered orthogonal frequency division multiplexing (F-OFDM) [8], [9] and filter bank multicarrier (FBMC) [10], [11], [12]. In [13], it is proved that the DCT-MCM is more robust than conventional OFDM schemes in terms of frequency offsets. These advantages make the DCT-MCM system as an attractive complementary candidate in future transmission schemes, especially for high mobility environments. Besides these benefits, when using DCT-MCM, instead of transmitting denser constellations at a subcarrier spacing of $1/T$, we can send the same amount of information by transmitting less dense, real-valued symbols at a subcarrier spacing of $1/(2T)$. Therefore, since typically the detection of less dense symbols is more robust to noise, DCT-MCM schemes can result in improved error-rate performance when operating far from the capacity limit.

However, one of the major practical challenges that DCT-MCM schemes encounter is that when DCT is used, the circular convolution property under multipath channels does not hold and, therefore the cyclic-prefix (CP) based approaches used in conventional OFDM systems [14], [15] do not apply. The properties of DCT have been studied in the seminal work in [16] and the one-tap equalization is applicable when the channel impulse response (CIR) is symmetric in time domain [14], [15]. In more generic wireless multipath fading channels, the condition for symmetric convolution between signals and CIR is not satisfied, and the channel cannot be compensated by simple one-tap equalizers exploiting cyclic prefixes. The problem of performing simple but efficient channel compensation and detection becomes even more challenging when adopting DCT-MCM together with MIMO employments.

In the literature, various attempts exist trying to address the symmetry issue. The method in [17], extends symmetrically the DCT processed signal, but the net data rate is, consequently, reduced by half. A more effective method is given by Al-Dhahir in [14] where one-tap equalization is enabled in the cosine domain, with the use of a time-domain finite impulse response (FIR) pre-filtering at the receiver so that CIR symmetry is rendered after filtering. However, this approach introduces doubled length overhead at transmitter. In addition, its combing with MIMO antenna technique requires a rigorous condition which the channel tap coefficients have to be real-valued. To the best of our knowledge, this is the first time that an efficient detection method is proposed that applies effectively to MIMO antenna DCT-MCM systems without harsh limitations on the channels. In this paper, we follow but go beyond the state of the art in [15] where zero padding is employed and at the receiver the DCT is replaced by a DFT of double the DCT length. This means that the $N$ subcarriers are demultiplexed by a DFT of $2N$ points, rather than using a $N$ point DCT. It is then examined that with useful information only kept on the in-phase branch, the inter-carrier-intereference (ICI) could be effectively eliminated by taking the real part of processed DFT outputs.

The remainder of the paper is organized as follows. We start in Section II by describing the transmission model of zero-padded DCT-MCM system. This is followed by a mathematical formulation of the corresponding detection problem. Section III examines three effective equalization/detection approaches for single-antenna systems and analytically compares their performance in terms of output SNR. Thereafter, the detection of MIMO DCT-MCM systems is addressed in Section IV, while the paper is concluded in Section V.

*Notations*: $[\cdot]^H$ and $[\cdot]^T$ stand for hermitian conjugate and transpose operation, respectively. $\mathbf{Re}\{\cdot\}$ and $\mathbf{Im}\{\cdot\}$ refer to the real and imaginary part taking operation. $\mathcal{F}_{2N}[\cdot]$ performs the DFT operation at length of $2N$. $E[\cdot]$ is defined as the expected value of random variable. We use $[\cdot]^*$ to return the conjugate of the identified element. A linear convolution operation of two vectors is denoted as $*$.

## II. System Description

In this section, we first describe the baseband model of a zero-padded DCT-MCM system over the wireless frequency-selective channel which is also illustrated in Fig. 1 [15]. While eight types of DCT [16] exist, we here consider the type-II DCT pair since it is the most often applied in practice [16]. For $N$ subcarriers carrying data information, the baseband modulated signal $x(n)$ can be represented as

$$x(n) = \sum_{k=0}^{N-1} a_k \beta_k \cos\Big[\frac{\pi k(2n+1)}{2N}\Big],\ n = 0, 1, \cdots, N-1. \quad (1)$$

where $a_k$ is amplitude-shift keying (ASK) modulated information symbol loaded on the $k$th subcarrier and with the parameter $\beta_k$ being defined as

$$\beta_k = \begin{cases} \sqrt{\frac{1}{N}}, & k = 0 \\ \sqrt{\frac{2}{N}}, & k = 1, 2, \cdots, N-1 \end{cases} \quad (2)$$

In order to achieve inter-symbol-interference free transmission, we insert zeros at the end of each block instead of symmetric prefix and suffix which is used as guard interval in pre-filtering methods [18]. Here, the CIR of a generic multipath complex channel is defined as $h(n)$ with length of $L$. Assuming that the guard interval length is identical to that of the channel, the zero-padded signal is, then, represented by $\tilde{x}(n)$, where $\tilde{x}(n) = x(n)$ for $0 \le n \le N-1$, and $\tilde{x}(n) = 0$ for $N < n \le N+L-1$. In this case, the received signal is obtained through the convolution with the channel as

$$r(n) = h(n) * \tilde{x}(n) + z(n), \quad 0 \le n \le N+L-1 \quad (3)$$

where $z(n)$ is the additive noise. At the receiver, the in-

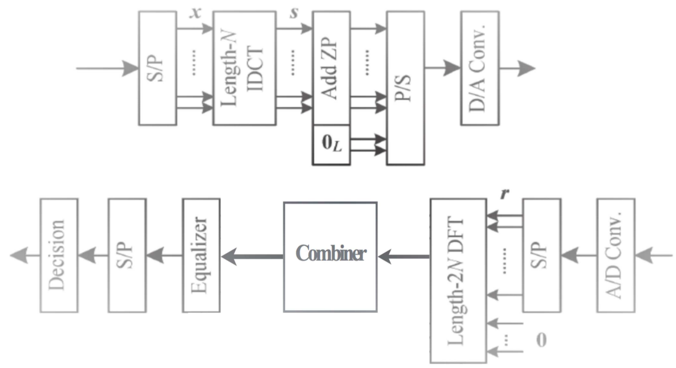


Fig. 1. Baseband equivalent model of zero-padded DCT-MCM system [15]

formation data extraction process is quite different from the conventional approach. We first complement zeros at the end of each received signal block to get a revised block of size $2N$. This effective received signal is denoted as $r_{2N}(n)$, where $r_{2N}(n) = r(n)$ for $0 \le n \le N+L-1$, and $r_{2N}(n) = 0$ for $N+L \le n \le 2N-1$. A length of $2N$ DFT operation is then performed to obtain the demultiplexed signal in frequency domain, which is

$$\begin{aligned} Y(m) &= \mathcal{F}_{2N}[r_{2N}(n)] \\ &= \mathcal{F}_{2N}[h_{2N}(n)] \cdot \mathcal{F}_{2N}[x_{2N}(n)] + \mathcal{F}_{2N}[z_{2N}(n)] \\ &= H(m) \cdot X(m) + Z(m),\ m = 0, 1, \cdots, 2N-1. \end{aligned} \quad (4)$$

where $h_{2N}(n)$ and $x_{2N}(n)$ are the zero padded blocks of length of $2N$ for $h(n)$ and $\tilde{x}(n)$, respectively. $z_{2N}$ is the zero padded counterpart of $z(n)$. To make the demodulated signal representation identical with DCT-II, without loss of generality, (4) can be modified to

$$\begin{aligned} Y(m) &= e^{j\frac{2\pi}{2N}m\cdot\frac{1}{2}} H(m) \cdot e^{-j\frac{2\pi}{2N}m\cdot\frac{1}{2}} X(m) + Z(m) \\ &= \tilde{H}(m) \cdot \tilde{X}(m) + Z(m) \end{aligned} \quad (5)$$

where $\tilde{H}(m) = e^{j\frac{2\pi}{2N}m\cdot\frac{1}{2}} H(m)$ and $\tilde{X}(m) = e^{-j\frac{2\pi}{2N}m\cdot\frac{1}{2}} X(m)$, respectively. As can be observed, the transmission channel effect can be eliminated by compensating for the term $\tilde{H}(m)$. Then, we need to focus further on $\tilde{X}(m)$ in order to identify effective equalization and detection algorithms. The demultiplexed signal $\tilde{X}(m)$ can be described as

$$\tilde{X}(m) = \sum_{k=0}^{N-1} a_k \cdot G(m,k) \quad (6)$$

with $G(m,k)$ being

$$G(m,k) = \sqrt{\frac{1}{2N}} \beta_k \sum_{n=0}^{N-1} \cos\frac{\pi}{N} k(n+\frac{1}{2}) \cdot e^{-j\frac{\pi}{N}m(n+\frac{1}{2})} \quad (7)$$

According to (7), the coefficient set $G(m,k)$ can get four kinds of values

$$G(m,k) = \begin{cases} \sqrt{\frac{1}{2}} & k=m, m=0 \\ 0.5 & k=m, 0<m\leq N-1 \\ -0.5 & k=2N-m, N<m\leq 2N-1 \\ j\mathbf{Im}\{G(m,k)\} & others. \end{cases} \quad (8)$$

Eq. (8) implies that all the useful information lies on the real part of demultiplexed signal $\tilde{X}(m)$ while the imaginary part accounts for interference. By combining (6) and (8), we yield

$$\tilde{X}(m) = \begin{cases} \sqrt{\frac{1}{2}}a_m & m=0 \\ 0.5a_m + j\cdot X_{I,m} & m=1,\cdots,N-1 \\ j\cdot X_{I,m} & m=N \\ -0.5a_{2N-m} + j\cdot X_{I,m} & m=N+1,\cdots,2N-1. \end{cases} \quad (9)$$

where $j\cdot X_{I,m}$ represents the integrated interference on the imaginary part from other subcarriers. From (9), we can equalize the first information symbol $a_0$ from the initial received symbol whereas the other information symbols from the rest subcarriers can be recovered either by equalizing the first half of $Y(m)$ at $m=1,\cdots,N-1$ or/and the other half of that at $m=N+1,\cdots,2N-1$, or by combining these two parts. For example, the information symbol $a_2$ lies on $\tilde{X}(m)$ at $m=2$ and $m=2N-2$. Consequently, the way to combine $\tilde{X}(2)$ and $\tilde{X}(2N-2)$ becomes the challenge for effectively recovering the data symbol $a_2$. It is noted that as the $N$th demultiplexed symbol $\tilde{X}(N)$ contains no useful information but only interference on the imaginary branch, we can safely neglect $Y(m)$ at $m=N$ in the following detection/equalization process.

## III. Equalization algorithms for zero-padded DCT-MCM

With double the demultiplexed symbols available, detection can be flexible and several combining techniques can be applied. In this paper, we reformulate three conventional combining schemes in an appropriate form for DCT-MCM and compare their superiority in terms of achievable output SNR.

### A. Uncombined Detection

Since the second half of the post-DFT demodulated signals repeats the same information, it is easy to use the first half symbols for equalization and neglect the others. Based on (5) and (9), the corresponding equalization process is represented by $\frac{Y(m)}{\tilde{H}(m)} = \sqrt{\frac{1}{2}}a_m + \frac{Z(m)}{\tilde{H}(m)}$ for $n=0$ and $\frac{Y(m)}{\tilde{H}(m)} = 0.5a_m + j\cdot X_{I,m} + \frac{Z(m)}{\tilde{H}(m)}$ for $n\neq 0$. We then take the real part of the equalized signal and the information data symbol is recovered as

$$\tilde{a}_m = \begin{cases} \frac{\sqrt{2}Y(m)}{\tilde{H}(m)} = a_m + \frac{\sqrt{2}Z(m)}{\tilde{H}(m)} & m=0 \\ \frac{2Y(m)}{\tilde{H}(m)} = a_m + \mathbf{Re}\{\frac{2Z(m)}{\tilde{H}(m)}\} & m=1,\cdots,N-1. \end{cases} \quad (10)$$

To derive the output SNR, we first assume that the normalized signal power of $a_k$ is $E_x$ and the noise variance of $Z(m)$ is $\sigma^2$. Accordingly, we have the output SNR for the several subcarriers to be

$$SNR_n^{UD} = \begin{cases} \frac{E_x|\tilde{H}(n)|^2}{2\sigma^2} & n=0 \\ \frac{E_x|\tilde{H}(n)|^2}{4\sigma^2} & n\neq 0. \end{cases} \quad (11)$$

It is noted that the first data information symbol is only kept by $\tilde{X}(m)$ at $m=0$, retaining the output SNR at the first subcarrier regardless of the equalization/combining scheme.

### B. Maximal ratio combining

In the above equalization/detection approach, we explore only the half or the post-DFT received signals for information recovery. However, this is clearly not the optimal solution as the half of received information is ignored. Maximal Ratio Combining (MRC) can be used to fully exploit all received elements and therefore maximize the output SNR [19]. The information signal from each desired symbol is rotated and compensated according to the phase and strength of the channel. The obtained signal is then in a combination of the two compensated symbols, which is

$$\begin{aligned} &\tilde{H}^*(m)Y(m) - \tilde{H}^*(2N-m)Y(2N-m) \\ &= \frac{|\tilde{H}(m)|^2 + |\tilde{H}(2N-m)|^2}{2}a_m \\ &+|\tilde{H}(m)|^2\cdot jX_{I,m} + |\tilde{H}(2N-m)|^2\cdot jX_{I,2N-m} \\ &+\tilde{H}^*(m)Z(m) - \tilde{H}^*(2N-m)Z(2N-m), m\neq 0 \end{aligned} \quad (12)$$

The interference from the term $X_{I,m}$ and $X_{I,2N-m}$ can be eliminated by taking the real operation:

$$\begin{aligned} &\mathbf{Re}\{\tilde{H}^*(m)Y(m) - \tilde{H}^*(2N-m)Y(2N-m)\} \\ &= \frac{|\tilde{H}(m)|^2 + |\tilde{H}(2N-m)|^2}{2}\cdot a_m + w_m^{MRC}, m\neq 0 \end{aligned} \quad (13)$$

where $w_m^{MRC} = \mathbf{Re}\{\tilde{H}^*(m)Z(m) - \tilde{H}^*(2N-m)Z(2N-m)\}$. The equalized symbol can, thus, be expressed as

$$\tilde{a}_m = \begin{cases} a_m + \frac{\sqrt{2}Z(m)\tilde{H}^*(m)}{|\tilde{H}(m)|^2} & m=0 \\ a_m + \frac{w_m^{MRC}}{|\tilde{H}(m)|^2+|\tilde{H}(2N-m)|^2} & m=1,\cdots,N-1. \end{cases} \quad (14)$$

The corresponding output SNR is expressed accordingly as

$$SNR_n^{MRC} = \begin{cases} \frac{E_x|\tilde{H}(n)|^2}{2\sigma^2} & n=0 \\ \frac{E_x(|\tilde{H}(n)|^2+|\tilde{H}(2N-n)|^2)}{4\sigma^2} & n\neq 0. \end{cases} \quad (15)$$

Compared with UD scheme, an diversity gain on output SNR is obtained for $n\neq 0$.

### C. Equal gain combining

In MRC scheme, the equalizer is build as a signal power combiner that is optimal in the sense of SNR. However, the technique requires the compensation weights to vary with the fading and the signals magnitude may fluctuate over several 10s of dB [20]. The equal gain combiner sidesteps this problem by setting unit gain at each element. In the equal gain combiner, we have equalized symbols at $m \neq 0$:

$$\frac{Y(m)}{\tilde{H}(m)} - \frac{Y(2N-m)}{\tilde{H}(2N-m)} = a_m + j(X_{I,m} - X_{I,2N-m}) + \frac{Z(m)}{\tilde{H}(m)} - \frac{Z(2N-m)}{\tilde{H}(2N-m)} \tag{16}$$

Similar to the MRC scheme, the real part of the combined signal is extracted to guarantee free interference condition, by which we have

$$\mathbf{Re}\{\tilde{H}^*(m)Y(m) - \tilde{H}^*(2N-m)Y(2N-m)\} = a_m + w_m^{EGC}, \quad m \neq 0 \tag{17}$$

where $w_m^{EGC} = \mathbf{Re}\{\frac{Z(m)}{\tilde{H}(m)} - \frac{Z(2N-m)}{\tilde{H}(2N-m}\}$. Also, the output SNR is given by

$$SNR_n^{EGC} = \begin{cases} \frac{E_x|\tilde{H}(n)|^2}{2\sigma^2} & n = 0 \\ \frac{E_x|\tilde{H}(n)|^2|\tilde{H}(2N-n)|^2}{(|\tilde{H}(n)|^2+|\tilde{H}(2N-n)|^2)\sigma^2} & n \neq 0. \end{cases} \tag{18}$$

### D. Performance comparison for the three schemes

With the output SNR derived we can evaluate each scheme's achieved performance. The first subcarrier achieves the same output SNR in all cases, or $SNR_n^{MRC} = SNR_n^{EGC} = SNR_n^{UD}$ for $n = 0$. For a fair comparison, we focus on the output SNR for the rest of the subcarriers. For the MRC and the EGC schemes we get

$$\begin{aligned} \frac{SNR_n^{MRC}}{SNR_n^{EGC}} &= \frac{(|\tilde{H}(n)|^2 + |\tilde{H}(2N-n)|^2)^2}{4|\tilde{H}(n)|^2|\tilde{H}(2N-n)|^2} \\ &= \frac{|\tilde{H}(n)|^4 + |\tilde{H}(2N-n)|^4}{4|\tilde{H}(n)|^2|\tilde{H}(2N-n)|^2} + \frac{1}{2} \\ &\geq \frac{2\tilde{H}(n)|^2|\tilde{H}(2N-n)|^2}{4|\tilde{H}(n)|^2|\tilde{H}(2N-n)|^2} + \frac{1}{2} = 1 \end{aligned} \tag{19}$$

Consequently, we have $SNR_n^{MRC} \geq SNR_n^{EGC}$ for $n \neq 0$. Similarly

$$\frac{SNR_n^{EGC}}{SNR_n^{UD}} = \frac{4|\tilde{H}(2N-n)|^2}{|\tilde{H}(n)|^2 + |\tilde{H}(2N-n)|^2} \tag{20}$$

In cases where the average channel power can be assumed equal among subcarriers (e.g. $E[|H(n)|^2] = E[|H(2N-n)|^2]$), as in the case of Rayleigh fading channel, then we can get that

$$\frac{E[SNR_n^{EGC}]}{E[SNR_n^{UD}]} = \frac{4E[(|\tilde{H}(2N-n)|^2)]}{2E[|\tilde{H}(2N-n)|^2]} = 2, \quad n \neq 0 \tag{21}$$

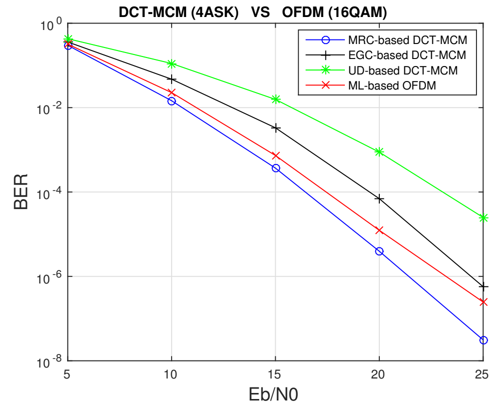


(a)

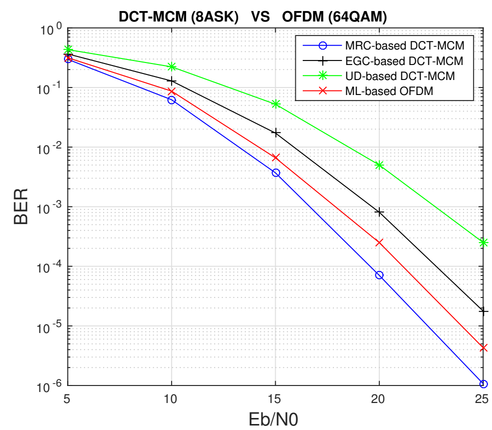


(b)

Fig. 2. BER comparison between DCT-MCM in three equalization schemes and ML-based OFDM system.(a)DCT-MCM(4ASK) VS OFDM(16QAM). (b)DCT-MCM(8ASK) VS OFDM(64QAM)

By taking the expected value of (19) and combines it with (21), we can have for our three schemes:

$$E[SNR_n^{MRC}] \geq E[SNR_n^{EGC}] = 2E[SNR_n^{UD}], \quad n \neq 0 \tag{22}$$

Fig. 2 gives the simulated bit-error rate (BER) performance of DCT-MCM systems with the three reformulated approaches, against a conventional maximum-likelihood (ML) employed OFDM based system under a ten-path slow-varying Rayleigh fading channel. Considering the subcarrier spacing in DCT-MCM is half of that in OFDM and one-dimensional signalling format is only allowed to keep subcarrier orthogonality on DCT-MCM, for a fair comparison, we assign 128 subcarriers to DCT-MCM with 4ASK scheme and 64 subcarriers to DFT-MCM with 16 quadrature amplitude modulation (16QAM) scheme respectively to obtain the same data rate within an allocated bandwidth. This principle is followed by the comparison for 8ASK modulated DCT-MCM and 64QAM modulated OFDM as well. In addition, the polynomial (133,171) code with constraint length of 7 and rate of 1/2 is employed for both systems. As can be seen from the figure, the MRC scheme can achieve the best performance for DCT-MCM systems, followed by EGC and UD schemes, which concurs with our output SNR analysis. In addition, the

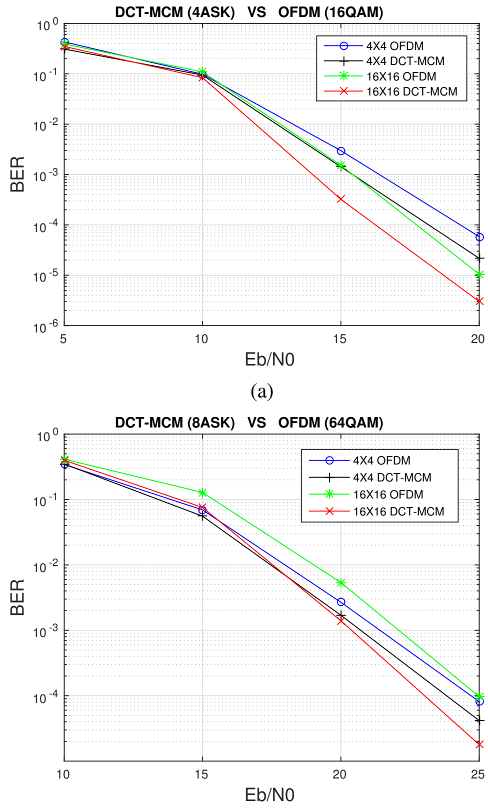


(a)

(b)

Fig. 3. BER comparison between DCT-MCM in EGC scheme and MMSE-based OFDM system in MIMO case. (a)DCT-MCM(4ASK) VS OFDM(16QAM). (b)DCT-MCM(8ASK) VS OFDM(64QAM)

OFDM system is only superior to the EGC and UD based DCT-MCM systems. By exploiting the diversity gain provided by double post-DFT symbols, the MRC-based DCT-MCM scheme can consistently outperform the conventional OFDM system by approximately 1.5 dB at a very low BER level.

## IV. Extension to MIMO system

The lack of circular convolution property by DCT also restricts the DCT-MCM employment with MIMO systems. For example, the pre-filtering method in [18] could sidestep the one-tap equalization problem. However, in MIMO scenarios such an approach is not efficient any more. In this section, we investigate the feasibility of the above three equalization schemes in combination with MIMO systems and the equalization process above is extended to matrix/vector forms accordingly as well.

We consider a typical MIMO case with $n_i$ inputs and $n_o$ outputs with zero-padded DCT-MCM. Without loss of generality, we can extend (5) into MIMO systems as

$$\mathbf{Y}_m = \tilde{\mathbf{H}}_m \cdot \tilde{\mathbf{X}}_m + \mathbf{Z}_m \tag{23}$$

where $\mathbf{Y}_m = [Y_1(m), Y_2(m), \dots, Y_{n_o}(m)]^T$ is the signal received vector and $\tilde{\mathbf{X}}_m = [\tilde{X}_1(m), \tilde{X}_2(m), \dots, \tilde{X}_{n_i}(m)]^T$ is the demodulated symbol vector, respectively. $\tilde{\mathbf{H}}_m$ can be viewed as a channel matrix of dimension $n_o \times n_i$ where its element $\tilde{H}_{i,j}(m)$ represents the channel frequency coefficient in the link from the $j$th transmitter to the $i$th receiver. Since the MRC provide better performance than the other two schemes, we consider it is as our first choice for DCT-MCM MIMO systems. The equalization process in (12) is, then, modified to

$$\begin{aligned}
&\tilde{\mathbf{H}}_m^H \mathbf{Y}_m - \tilde{\mathbf{H}}_{2N-m}^H \mathbf{Y}_{2N-m} \\
&= \frac{\tilde{\mathbf{H}}_m \tilde{\mathbf{H}}_m^H + \tilde{\mathbf{H}}_{2N-m} \tilde{\mathbf{H}}_{2N-m}^H}{2} \mathbf{A}_m \\
&+ \tilde{\mathbf{H}}_m \tilde{\mathbf{H}}_m^H \cdot j\mathbf{X}_{I,m} + \tilde{\mathbf{H}}_{2N-m} \tilde{\mathbf{H}}_{2N-m}^H \cdot j\mathbf{X}_{I,2N-m} \\
&+ \tilde{\mathbf{H}}_m^H \mathbf{Z}_m - \tilde{\mathbf{H}}_{2N-m}^H \mathbf{Z}_{2N-m}, \quad m \neq 0
\end{aligned} \tag{24}$$

where $\mathbf{A}_m = [a_1^m, a_2^m, \dots, a_{n_i}^m]^T$ is the data information vector at $m$th subcarrier and $\mathbf{X}_{I,m}$ is the vectored counterpart for the interference $X_{I,m}$. As can be seen from (24), the equalized interference terms $\tilde{\mathbf{H}}_m \tilde{\mathbf{H}}_m^H \cdot j\mathbf{X}_{I,m}$ and $\tilde{\mathbf{H}}_{2N-m} \tilde{\mathbf{H}}_{2N-m}^H \cdot j\mathbf{X}_{I,2N-m}$ are now complex, with both real and imaginary parts, resulting in unavoidable crosstalk to the data information vector. However, this does not hold for the EGC and the UD schemes. In the equal gain combiner case, we have the following derivations for $m \neq 0$

$$\begin{aligned}
&\frac{\mathbf{Y}_m}{\tilde{\mathbf{H}}_m} - \frac{\mathbf{Y}_{2N-m}}{\tilde{\mathbf{H}}_{2N-m}} = \\
&\mathbf{A}_m + j(\mathbf{X}_{I,m} - \mathbf{X}_{I,2N-m}) + \frac{\mathbf{Z}_m}{\tilde{\mathbf{H}}_m} - \frac{\mathbf{Z}_{2N-m}}{\tilde{\mathbf{H}}_{2N-m}},
\end{aligned} \tag{25}$$

Still, the interference term $j(\mathbf{X}_{I,m} - \mathbf{X}_{I,2N-m})$ has only an imaginary part, allowing for interference free detection. Since the EGC scheme typically achieves better performance than the UD one as verified in (22), we take it as priority choice for MIMO detection. Then, the recovered symbol vector $\tilde{\mathbf{A}}_m$ is provided as

$$\tilde{\mathbf{A}}_m = \begin{cases} \mathbf{A}_m + \frac{\sqrt{2}\mathbf{Z}_m}{\tilde{\mathbf{H}}_m} & m = 0 \\ \mathbf{A}_m + \mathbf{Re}\{\frac{\mathbf{Z}_m}{\tilde{\mathbf{H}}_m} - \frac{\mathbf{Z}_{2N-m}}{\tilde{\mathbf{H}}_{2N-m}}\} & m = 1, \cdots, N-1. \end{cases} \tag{26}$$

Fig. 3 shows the BER for EGC-based DCT-MCM and $4 \times 4$ and $16 \times 16$ MIMO chahnnels. The performance of MIMO-OFDM system is also provided for comparison. Due to the impractical complexity of ML detection, we instead apply a minimum mean square error (MMSE) equalizer which is of similar computational complexity to the EGC scheme. The simulation assumptions of the former Section are also adopted here. With our proposed detection methods, DCT-MCM schemes show improved error rate performance than the conventional MIMO-OFDM system for both the $4 \times 4$ and $16 \times 16$ cases.

## V. Conclusion

In this paper, we examined several equalization/detections schemes for zero-padded DCT-MCM systems. Their corresponding output SNR is derived and compared. It has been shown that for single antenna systems, MRC is the optimum approach for DCT-MCM and can outperform traditional OFDM systems. However, tis extension to MIMO scenario is prohibited from interference related problems. Nevertheless, our simulation results show the EGC based detection approach can be a good candidate for DCT-MCM MIMO systems and can outperform MIMO-OFDM systems employing MMSE detection.

## References


[1] M. Rodrigues and I. Darwazeh, "Fast OFDM: A proposal for doubling the data rate of OFDM schemes", *IEEE/IEE International Conference on Telecommunications*, 2002.

[2] S. Parkvall E. Dahlman and J. Skold, "4G: LTE/LTE-advanced for mobile broadband", *Academic Press*, 2011.

[3] P. Xiao, C. Toal, D. Burns, V. Fusco, and C. Cowan, "Transmit and receive filter design for OFDM based WLAN systems", in *2010 International Conference on Wireless Communications Signal Processing (WCSP)*, Oct 2010, pp. 1–4.

[4] L. Wen, R. Razavi, M. A. Imran, and P. Xiao, "Design of joint sparse graph for OFDM system", *IEEE Transactions on Wireless Communications*, vol. 14, no. 4, pp. 1823–1836, April 2015.

[5] G. Fettweis, M. Krondorf, and S. Bittner, "GFDM - generalized frequency division multiplexing", in *VTC Spring 2009 - IEEE 69th Vehicular Technology Conference*, April 2009, pp. 1–4.

[6] L. Zhang, A. Ijaz, P. Xiao, A. Quddus, and R. Tafazolli, "Subband filtered multi-carrier systems for multi-service wireless communications", *IEEE Transactions on Wireless Communications*, vol. 16, no. 3, pp. 1893–1907, March 2017.

[7] L. Zhang, P. Xiao, and A. Quddus, "Cyclic prefix-based universal filtered multicarrier system and performance analysis", *IEEE Signal Processing Letters*, vol. 23, no. 9, pp. 1197–1201, Sept 2016.

[8] L. Zhang, A. Ijaz, P. Xiao, and R. Tafazolli, "Multi-service systems: An enabler of flexible 5G air-interface", *IEEE Communications Magazine*, to appear, 2017.

[9] L. Zhang, A. Ijaz, P. Xiao, A. Quddus, and R. Tafazolli, "Single-rate and multi-rate multi-service systems for next generation and beyond communications", in *2016 IEEE 27th Annual International Symposium on Personal, Indoor, and Mobile Radio Communications (PIMRC)*, Sept 2016, pp. 1–6.

[10] L. Zhang, P. Xiao, A. Zafar, A. u. Quddus, and R. Tafazolli, "FBMC system: An insight into doubly dispersive channel impact", *IEEE Transactions on Vehicular Technology*, vol. 66, no. 5, pp. 3942–3956, May 2017.

[11] J. Du, P. Xiao, J. Wu, and Q. Chen, "Design of isotropic orthogonal transform algorithm-based multicarrier systems with blind channel estimation", *IET Communications*, vol. 6, no. 16, pp. 2695–2704, November 2012.

[12] R. Razavi, P. Xiao, and R. Tafazolli, "Information theoretic analysis of ofdm/oqam with utilized intrinsic interference", *IEEE Signal Processing Letters*, vol. 22, no. 5, pp. 618–622, May 2015.

[13] P. Tan and N. C. Beaulieu, "A comparison of DCT-based OFDM and DFT-based OFDM in frequency offset and fading channels", *IEEE Transactions on Communications*, pp. 2113–2125, Nov 2006.

[14] N. Al-Dhahir, H. Minn, and S. Satish, "Optimum DCT-based multicarrier transceivers for frequency-selective channels", *IEEE Transactions on Communications*, vol. 54, no. 4, pp. 760–760, April 2006.

[15] X. Ouyang and J. Zhao, "Single-tap equalization for fast OFDM signals under generic linear channels", *IEEE Communications Letters*, vol. 18, no. 8, pp. 1319–1322, Aug 2014.

[16] V. Sanchez, P. Garcia, A. M. Peinado, J. C. Segura, and A. J. Rubio, "Diagonalizing properties of the discrete cosine transforms", *IEEE Transactions on Signal Processing*, pp. 2631–2641, Nov 1995.

[17] G. D. Mandyam, "Sinusoidal transforms in OFDM systems", *IEEE Transactions on Broadcasting*, vol. 50, no. 2, pp. 172–184, June 2004.

[18] Chang He, L. Zhang, J. Mao, Aijun Cao, P. Xiao, and M. A. Imran, "Output SNR analysis and detection criteria for optimum DCT-based multicarrier system", in *2016 International Symposium on Wireless Communication Systems (ISWCS)*, Sept 2016, pp. 59–64.

[19] T. Eng, Ning Kong, and L. B. Milstein, "Comparison of diversity combining techniques for rayleigh-fading channels", *IEEE Transactions on Communications*, vol. 44, no. 9, pp. 1117–1129, Sep 1996.

[20] D. Hamza, S. Assa, and G. Aniba, "Equal gain combining for cooperative spectrum sensing in cognitive radio networks", *IEEE Transactions on Wireless Communications*, vol. 13, no. 8, pp. 4334–4345, Aug 2014.